ACADEMIA ROMÂNĂ
Revue Roumaine de Chimie
http://web.icf.ro/rrch/

Rev. Roum. Chim.,
2018, *63*(9), 837-845

Dedicated to Niculae I. Ionescu PhD
on the occasion of his 85th anniversary

ENHANCED PHOTOCATALYTIC ACTIVITY OF ZnO NANOPARTICLES OBTAINED BY "GREEN" SYNTHESIS WITH WELL DISPERSED Pd-Au BIMETALLIC NANOPARTICLES

Mariana CHELU, Razvan STATE, Cornel MUNTEANU, Irina ATKINSON, Adriana RUSU, Veronica BRATAN, Adina MUSUC, Ioan BALINT and Florica PAPA*

"IlieMurgulescu" Institute of Physical Chemistry, Roumanian Academy, 202 Splaiul Independentei, 060021 Bucharest, Roumania

Received July 31, 2017

The aim of this work is to study the photocatalytic reduction of nitrate in drinking water using ZnO nanoparticles comparative with bimetallic Pd-Au nanoparticles loaded ZnO and formic acid as a hole scavenger. ZnO nanostructured materials are promising photocatalysts because of their non toxicity, low cost and good stability. Noble metals (Au, Ag, Pd) supported by ZnO have attracted significant interest, as it may possibly result in a superior photocatalytic activity.

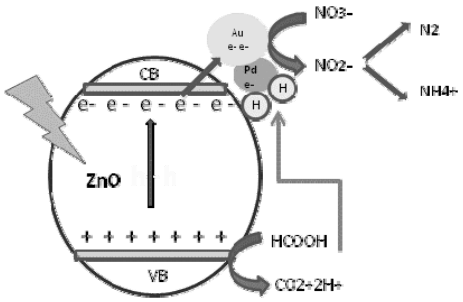

The ZnO nanoparticles were obtained with the extract of black tea solid waste and Zn acetate dehydrate in alkaline medium. Bimetallic nanoparticles Pd-Au of around 10 nm were obtained through a green chemistry method by adding a solution containing the gold precursor ($HAuCl_4$) and paladium precursor $Pd(NO_3)_2$ in a tannic acid solution. The surface and chemical state analysis of pure ZnO and Pd-Au deposited ZnO were investigated by XRD, SEM-EDX, TEM, IR-spectroscopy and UV-Vis spectroscopy. The photocatalytic activities were evaluated by nitrate reduction reactions in aqueous solutions. The Hg lamp of 120 W was used as a source for photocatalytic study. Compared with ZnO nanoparticles, Pd-Au loaded (1% weight) on ZnO catalyst shows an increased catalytic activity, which has been evaluated in terms of N_2 selectivity.

INTRODUCTION

The NO_3^- is a compound dangerous to human health because it can turn into nitrite in the human body and may drive different diseases: endocrine disruptor, blue baby syndrome, gastrointestinal cancer, etc. The nitrate removal by conventional water treatment methods is very difficult due to the compound's high solubility and stability, co-precipitation and adsorption properties. One of the most important environmental issues is the ground water nitrate pollution resulting from intense fertilization, animal waste and industrial effluents.

The World Health Organization has set the maximum contaminant level to 50 mg/L for NO_3^-, 0.5 mg/L for NO_2^- and 0.5mg/L for NH_4^+ in drinking water.

Research efforts are directed towards reducing nitrates selectively into nitrogen for water purification.

Photocatalysts of semiconductor type are promising materials for removal of pollutants in air and in water, because of their capacity to produce photogenerated conduction band electrons and

* Corresponding author: frusu@icf.ro

valence band holes, which enable redox reactions with adsorbed aqueous species. Numerous studies report synthesis of new photocatalysts for nitrate reduction in drinking water systems. [1,2]

Recently, the green chemistry approach for nanoparticles synthesis receives more attention due to its eco-friendliness, cost-effectiveness and sustainability. Plant materials have been extensively used for a variety of metal and metaloxide nanoparticle synthesis due to their numerous phytochemicals, including alkaloids, polyphenols, carotenoids, polysaccharides, lectins and terpenes.[3]

The use of plant extract as an economic and effective alternative represents an interesting, fast and clean synthetic route for the large scale synthesis of semiconductor materials such as ZnO.

Semiconductor–metal heterostructured nanomaterials have attracted great interest in recent years because they can not only combine the unique properties of metals and semiconductors, but also generate novel electrical, optical, and catalytic properties due to the synergetic interaction between the metal and the semiconductor components.

The photoreduction of nitrate by metal catalyst supported on semiconductor has been reported in many papers, TiO_2,[1,4] ZnS,[5] ZnO.[6,7]

ZnO has been widely investigated as a promising material because of its photocatalytic activity, good photostability, low price and ecological sustainability.[8,9] On the other hand, pure ZnO usually reveals low photo-energy conversion because of the relatively low charge carrier separation competence and fast recombination of charge carriers.

Noble metal nanoparticles deposition on ZnO have been shown to enhance the photocatalytic properties of ZnO by: i) facilitating the formation of electron/hole pairs induced by the surface plasmon resonance (SPR) effect, ii) increasing the competence of charge carrier separation and iii) extending light absorption.[10] Stored electrons in the metal nanoparticles will then be available for nitrate reduction. Moreover, the presence of hole scavengers normally increases the efficiency of the process by avoiding the recombination of electron and holes.

In this work, we investigated the photocatalytic activity of ZnO nanopowder synthesized through the green method and we compared with supported bimetallic nanoparticles Pd-Au loading ZnO nanoparticles for photocatalytic nitrate reduction reaction. The effect of formic acid as the reductant and/or hole scavenger was investigated under similar reaction conditions.

EXPERIMENTAL

The ZnO catalysts have been synthetized through a green chemistry method. The synthesis of ZnO green materials is adapted from methods described by Saad *et al.*[11]
Pd-Au bimetallic nanoparticles were obtained in a green way adding a solution containing the gold and palladium precursor in a tannic acid solution.

Materials

Zinc acetate dihydrate $Zn(CH_3COO)_2$-$2H_2O$ (99.7%), Merck, deionized water, black tea extract, palladium nitrate solution, Pd 8.5% w/w Alfa-Aesar, sodium hydroxide anhydrous, (97%) Alfa-Aesar, tetrachloroauric acid (III) trihydrate, 99.5%, $AuHCl_4$ $3H_2O$, tannic acid, Carl Roth (86%).

Synthetization and characterization of zinc oxide nanoparticles

Preparation of the extract

The mixture of 2grams of dried black tea solid waste and 100 mL of distilled water have been gently warmed up until the solution turned dark red. The black tea extract contains water-soluble phytochemicals (flavones, quinones and organic acids etc.) which has a strong reductive character in alkaline medium.

3 grams of Zn acetate dihydrate has been dissolved in distilled water by vigorously stirring for 10 minutes. 15 mL of filtered black tea extract was added to the Zn acetate solution. NaOH was added dropwise, with continuous stirring. The mixture was slowly stirred for 2 hours to obtain the precipitate of ZnO nanoparticles. The pale white precipitate that was obtained was collected and washed several times with distilled water and ethanol. Each washing step was followed by centrifuge. The obtained product was dried at 90^{o}C for 20 hours.Therefore, it is suggested that water soluble phytochemicals of tea extract have an important role in the total process of obtaining ZnO nanoparticles.

Bimetallic nanoparticles of around 10 nm were obtained in a green chemistry method by added dropwise with stirring a solution containing the gold precursor ($HAuCl_4$ $3H_2O$), 0.9 mM and palladium precursor $Pd(NO_3)_2$ 0.9 mM in a tannic acid solution.[12] The molar ratio between Pd : Au was 1:1.The photocatalyst Pd-Au/ZnO was obtained by dispersing the nanoparticles, previously dissolved by sonication in deionized water on ZnO. The bimetallic nanoparticles were dried at 100^{o}C for 2 h and then calcined at 300^{o}C for 1 h. The final metal loading of support oxides was 1 wt%.

Characterization

The morphology of the powders was obtained by scanning electron microscopy (SEM) using FEI Quanta 3D FEG instrument at an accelerating voltage of 5 kV, in high-vacuum mode with Everhart–Thornley secondary electron (SE) detector coupled with EDX analysis.

ZnO and Pd-Au/ZnO deposition were investigated by transmission electron microscopy (TEM) performed on FEI Tecnai G2-F30 S-Twin field-emission gun scanning transmission electron microscope (FEG STEM) operating at 300 kV. A drop of the nanoparticles suspension was mounted on a holey carbon film copper grid allowing the solvent to evaporate at room temperature. XRD measurements were performed with Ultima IV X-Ray Diffractometer (Rigaku Japan) operated at 40 kV and 30mA using Cu Kα radiation (Kα = 1.54 Å) with a scan rate of 5^{0}C/min and 0.02^o step size. The XRD diffractograms were collected between 10^0 and 80^0.

Thermal measurements were performed in air atmosphere with a Netzch STA 449 F1 Jupiter simultaneous thermal analyzer at a heating rate of 5°C/min, in the 25 – 1000°C temperature range.

The FT-IR spectra were recorded at the wavenumber range of 400 to 4,000 cm^{-1} using FT-IR Spectroscopy with a Nicolet 6700 apparatus.

UV-VIS spectra were collected by a Perkin Elmer Lambda 35 spectrophotometer equipped with integrating sphere. The measurements were performed in the range 200-1100 nm, using spectralon as reference. The reflectance measurements were converted to absorption spectra using the Kubelka-Munk function, F(R). The absorbance F(R) can be expressed as $F(R) = (1 - R)^2/2R$, where R represents the diffuse reflectance from a semi-infinite layer.

The photocatalysts performance of ZnO NPs and Pd-Au/ZnO deposition in the nitrate reduction reaction was evaluated in the absence and presence of the formic acid as the reductant and/or hole scavenger in the photochemical reactor made of quartz (Photochmical Reactors LTD). For each experiment, 70 mL NO_3^- solution with the initial aqueous nitrate concentrations of 1.61 mmol/L were agitated with the 0.03 g photocatalyst. The molecular ratio of electron sacrificial donor HCOOH : NO_3^- was 1:1. The photochemical reactor was irradiated with a 125 W medium pressure mercury lamp. The lamp radiates largely in the 366 nm wavelength, as well as in the visible region (404–579 nm) with slighter in the ultraviolet region (265–334 nm). The samples were continuously purged with flow of Ar to eliminate any dissolved oxygen. Prior to irradiation, the suspension was kept on stirring at 18°C to minimize the temperature increase in nitrate solution under the UV illumination. The concentration of nitrate, nitrite, ammonium and formic acid in the solution after the photocatalytic reduction was thoroughly analyzed using ion-chromatogram ISC-900 Dionex.The nitrogen, which is a gaseous product, was calculated from the mass balance of reaction.

RESULTS AND DISCUSSION

Characterization of green synthesized ZnO nanoparticles

TEM techniques were employed to visualize the morphologies and size of the nanoparticles that formed. The TEM images recorded from Pd-Au nanoparticles are shown in Fig. 1.a. The microscopy images show the presence of well-defined particles with a predominant rounded shape, with the diameter of most of the particles in the range of 7-10 nm (Figure 1a).

The TEM images of catalysts ZnO support show good dispersion with a particle size in the range >100nm (Figure 1b).

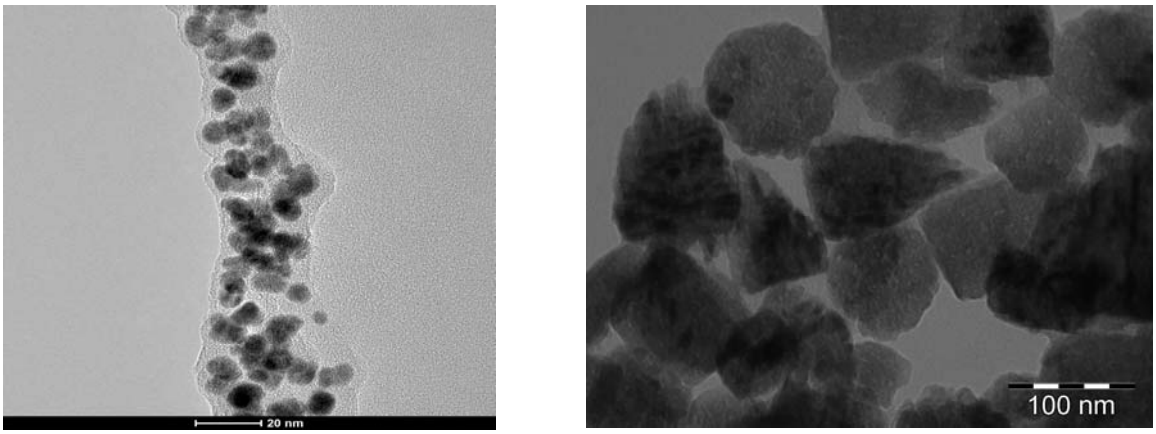

a b

Fig. 1 – TEM images of Pd-Au NPs (a) and ZnO NPs (b).

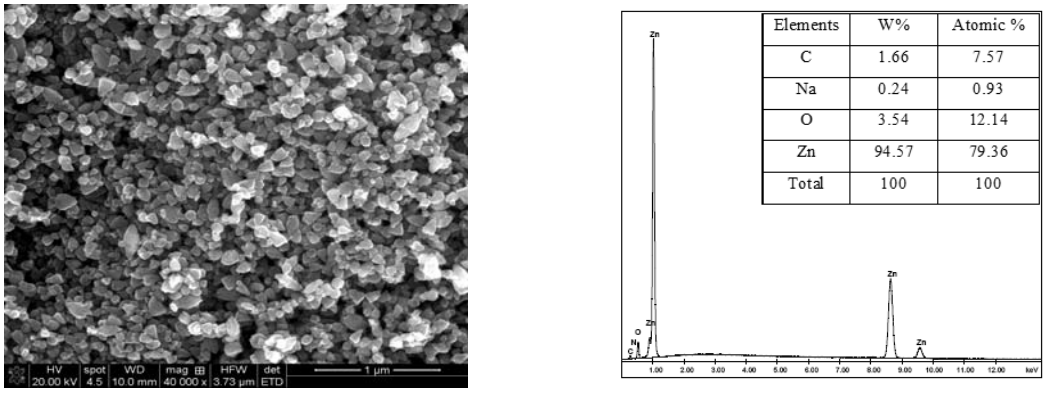

Elements	W%	Atomic %
C	1.66	7.57
Na	0.24	0.93
O	3.54	12.14
Zn	94.57	79.36
Total	100	100

a b

Fig. 2 – SEM image for ZnO (a), EDAX for ZnO quantification (element normalized) (b).

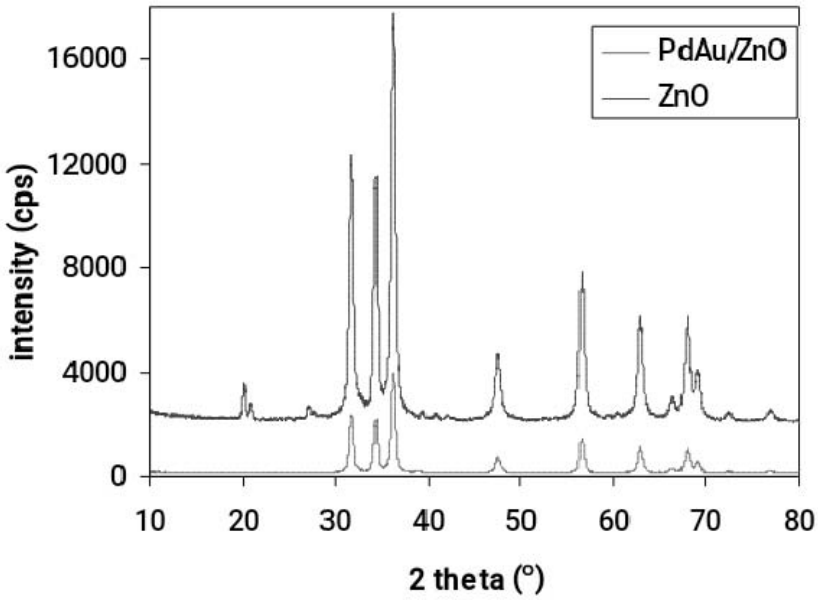

Fig. 3 – XRD spectra of ZnO and Pd-Au/ZnO materials.

The XRD patterns of ZnO and Pd-Au/ZnO nanoparticles are presented in Figure 3. The diffraction peaks observed at: 31.72^0, 43.37^o, 36.20^0, 47.47^0, 56.56^0, 62.78^0, 66.26^0, 67.92^0, 69.02^0, 72.51^0, 76.89^0 are identical to ZnO planes of (100), (002), (101), (102), (110), (103), (200), (112), (201). The observed XRD patterns peaks (Figure 3) represent the wurtzite phase of ZnO, which is consistent with the standard card (JCPDS No. 36-145) with lattice constants of a = b = 0.3252 nm, c = 0.52103 nm.

Thermal analysis technique was used to study how a material's heat capacity (Cp) is changed by temperature. Figure 4b) is the DSC curve characterization based on ZnO nanomaterials. Based on the DSC, the TG analysis of ZnO nanoparticles (Figure 4a) shows a 4.14% total weight loss. The first weight loss on TG curve (approximately 2%) (T_{DTG} = 128°C) is due to the loss of water and is associated with an endothermal effect on DSC curve (Figure 4b) at T_{min} = 129° C. The continuous weight loss between 160 and 380°C (T_{DTG} = 215.5°C) could be ascribed to the loss of other volative components in the black tea extracts used as reduction and stabilization agent.

The thermal analysis of Pd-Au/ZnO shows a good stability of nanoparticles in the investigated temperature range, between 30 and 1000°C. The mass loss of 2% (Figure 4b) (T_{DTG} = 399°C) is associated with a small exothermal peak on DSC curve (Figure 4b) centered at T_{max} = 404°C, which is related to the remaining fragments containing CH groups from the preparation method.

Infrared spectroscopy was used to detect the presence of functional groups adsorbed on the surface of synthetized nanoparticles. Figure 5 represents the FT-IR spectra of ZnO and Pd-Au/ZnO obtained from green method acquired in the range of 500 – 4000 cm^{-1}. The absorption peak was observed in the range of 3000-3600 cm^{-1}. This was centered at 3445 cm^{-1} corresponding to the stretching vibration of intermolecular hydrogen bond (O-H), existing between adsorbed molecular water and indicates the higher amount of hydroxyl groups. Two bands at 2925 and 2842 cm^{-1} corresponding to the C-H stretching modes are presented. A sharp absorption at 1621 cm^{-1} is assigned to the O-H stretching vibrations from Zn-OH bonds, and other (small) bands at 1379 and 887 cm^{-1} and 712 cm^{-1} is characteristic to N-O symmetric stretch.[13] The spectrum obtained in FT-IR images shown that the characteristic absorption peaks of Zn-O are nearer to 470 cm^{-1} and confirms the presence of ZnO.

UV-visible absorption spectroscopy is a technique that is widely being used to examine the optical properties of nanosized particles. The absorption spectrum of ZnO and Pd-Au/ZnO deposition materials is shown in Figure 6. It exhibits a strong absorption band at about 360 (ZnO) and 380 nm (Pd-Au/ZnO). This can be assigned to the intrinsic band gap absorption of

ZnO due to the electron transitions from the valence band to the conduction band. Pd-Au/ZnO nanoparticles show a broad absorption starting at 390 nm. This band appears due to the superposition of the PdO absorption, at ~ 470 nm,[14] and of the surface plasmon resonance band at ~550 nm characteristic of gold nanoparticles.[15] The small shoulder appeared at ~210 nm could be assigned to the presence of palladium nanoparticles.[16]

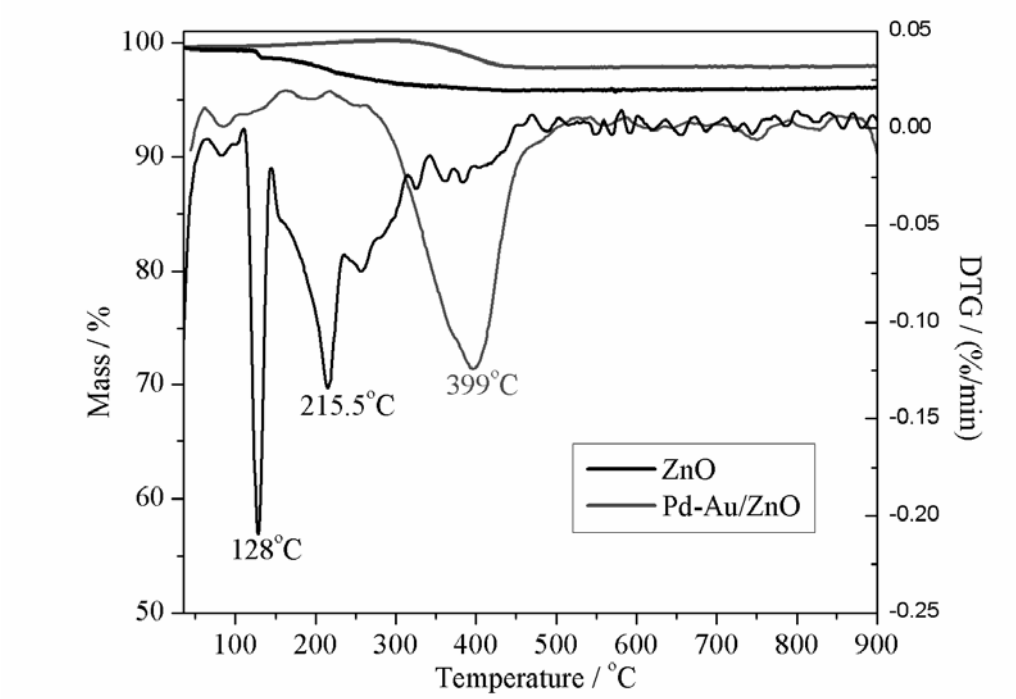

Fig. 4 – DSC (a) and TG-DTG (b) thermograms.

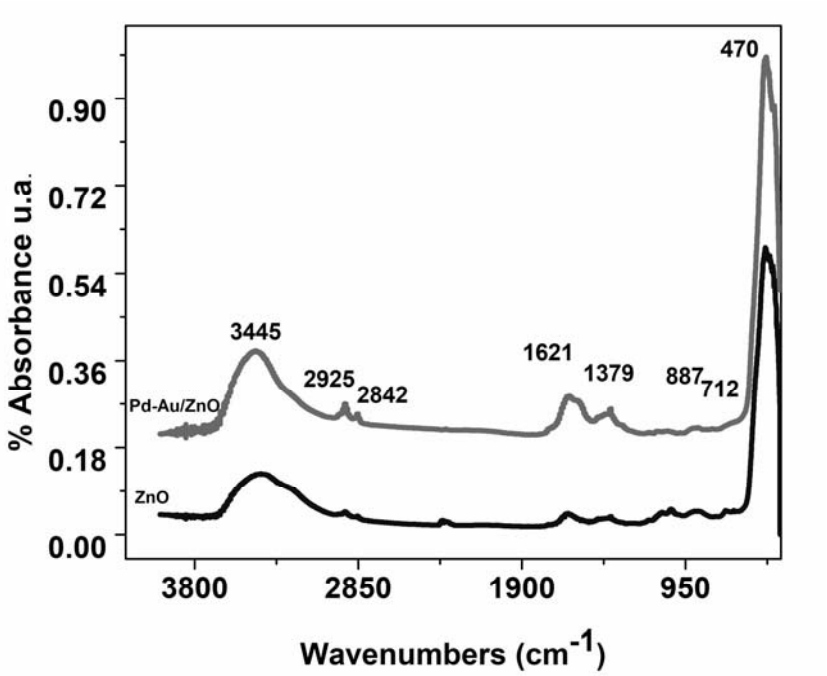

Fig. 5 – FT-IR spectra for ZnO and Pd-Au/ZnO.

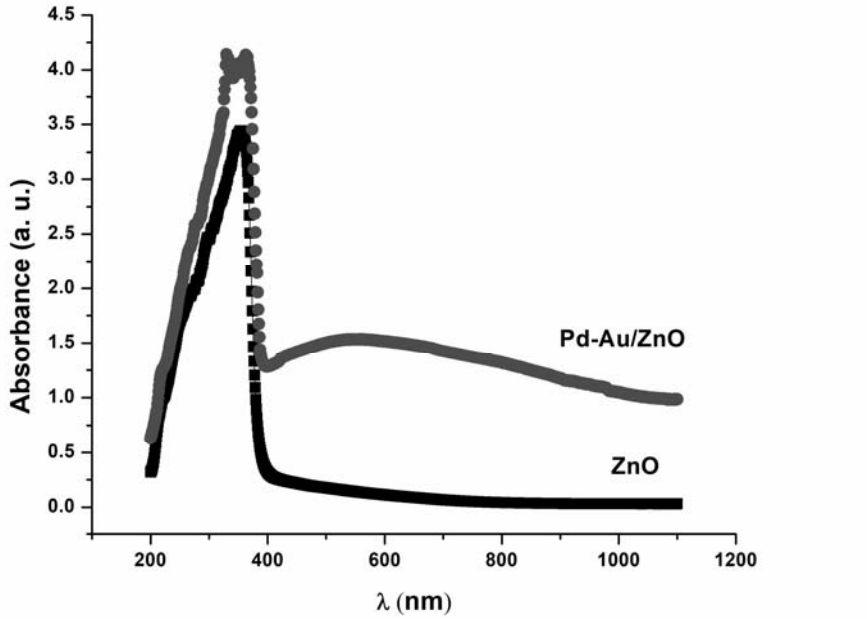

Fig. 6 – UV- visible absorption spectra.

Photocatalytic test for nitrate reduction

The time-dependence concentration of photocatalytic reduction of the 1.6 mmol/L (100 mg/L) nitrate under irradiation of UV lamp on the pure ZnO NPs and Pd-Au/ZnO in the absence and presence of formic acid as reductant and/or hole scavenger is revealed in Figure 7.

As it can be seen from Figure 7, both ZnO NPs and Pd-Au/ZnO have a good efficiency in nitrate removal. In the absence of formic acid the nitrate is converted to nitrite according to the reaction (1):

$$NO_3^- + 2e^- + 2H^+ \rightarrow NO_2^- + H_2O \qquad (1)$$

Production of nitrite or ammonia in drinking water as secondary product is undesirable.

By adding the hole scavenger it improves nitrate and nitrite reduction, but it is inconvenient because it increases the amount of ammonium, unwanted product in drinking water.

Therefore, formic acid does not act as a direct reductant under experimental conditions, the addition of formic acid provides the hydrogen necessary for the reduction of NO_2^- to N_2 and NH_4^+ according to the equations (2), (3), thus, the formic acid (HCOOH) could be decomposed into H_2 and CO_2 by the catalyst which produces in situ H_2 (as suggested in Scheme 1), necessary in nitrate reduction reaction .[17,18]

The CO_2 results act as buffer to stabilize the pH of solution of the photocatalytic reaction.[19]

The pH of the nitrate solution in the presence of 0.008 M formic acid was 3.7.

$$2\,NO_2^- + 6e^- + 8H^+ \rightarrow N_2 + 4H_2O \qquad (2)$$

$$2\,NO_2^- + 6e^- + 8H^+ \rightarrow NH_4 + 2H_2O \qquad (3)$$

Generally, loading noble metals of semiconductor photocatalysts is necessary for enhancing the photocatalytic performance and N_2 selectivity.[20] The semiconductor photocatalysts like TiO_2, ZnS, and ZnO show photocatalytic activity performance when these photocatalysts are modified with bimetals, Pd-Cu,[1] Fe-Pd,[21] Pd-Au.[22] ZnO modified with the Pd-Au bimetallic nanoparticles generates electrons in the semiconductor by UV irradiation should be transferred to the metal nanoparticles where they then reduce NO^{3-} with H^+, which are adsorbed on the surface of the metal particles. According to this mechanism, the metal particles should have the ability to show high photocatalytic performance by improved rate of trapping photoexcited electrons and inhibited recombination due to the capability of storage of photoexcited electrons using bimetallic nanoparticles. Soares *et al.*[1] reported that the photogenerated holes in the valence band can be consumed by formic acid to form CO_2, which has a strong reductive ability and tends to reduce nitrate to nitrogen.

Bimetallic Pd-Au nanoparticles exhibit the plasmon resonance on the surface, as can be seen in figure 6. The plasmonic effect has a main contribution to improving the photocatalytic activity of zinc oxide loaded with Pd-Au 1%.

The possible mechanism involved in the reduction of nitrate for Pd-Au NPs/ ZnO was illustrated in the Scheme 1.

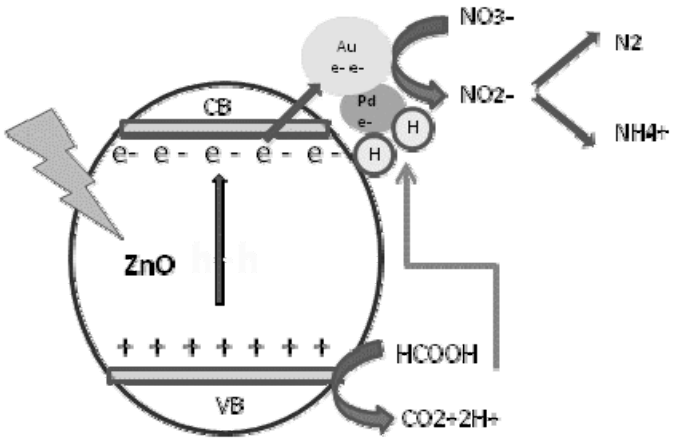

Scheme 1 – Possible mechanism for photocatalytic nitrate reduction on Pd-Au/ZnO catalyst.

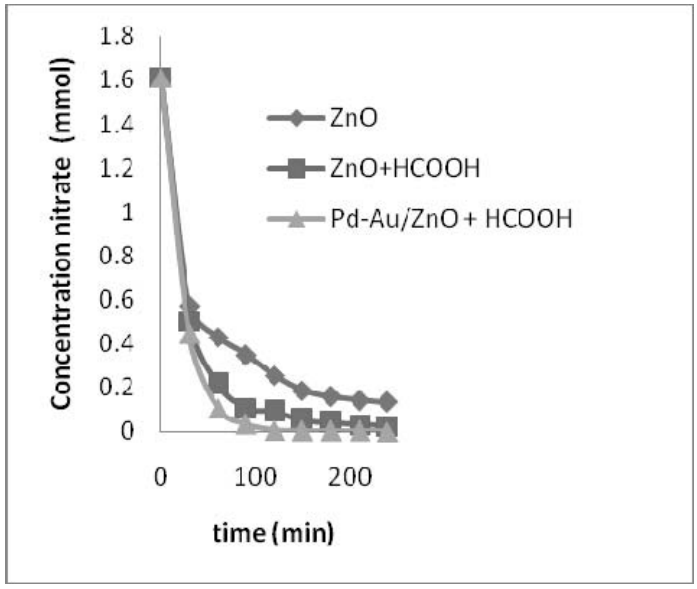

Fig. 7 – Time dependence of photocatalytic activity on ZnO and Pd-Au/ ZnO.

The effect of the formic acid and Pd-Au loaded ZnO on the nitrate conversion and selectivity to nitrite, ammonium and nitrogen, obtained in the photocatalytic nitrate reduction, is presented in Fig. 8.

As can be observed in Fig. 8, the presence of a scavenger improves the photocatalytic process and N2 selectivity.

The selectivity to nitrite and ammonium was calculated as:

$$S(NO_2^-)\% = [NO_2^-]_{240}/([NO_3^-]_i - [NO_3^-]_{240}) * 100 \quad (4)$$

$$S(NH_4^+)\% = [NH_4^+]_{240}/([NO_3^-]_i - [NO_3^-]_{240}) * 100 \quad (5)$$

$$S(NO_3^-)\% = [NO_3^-]_{240}/([NO_3^-]_i - [NO_3^-]_{240}) * 100 \quad (6)$$

where $[NO_3^-]_i$ is the concentration before irradiation and $[X]_{240}$ is the concentration at time = 240 min.

The amounts of nitrogen were calculated by a mole balance, assuming that the amount of NO_x produced is negligible.

Compared with ZnO, bimetal Pd-Au loaded catalysts have shown excellent selectivity to N_2 in the photocatalytic reduction of nitrate in the presence of formic acid. The highest photocatalytic activity and selectivity to N_2 is achieved by using Pd-Au/ZnO catalyst with 1:1 metal molar ratio and 1 wt.% total metal content.

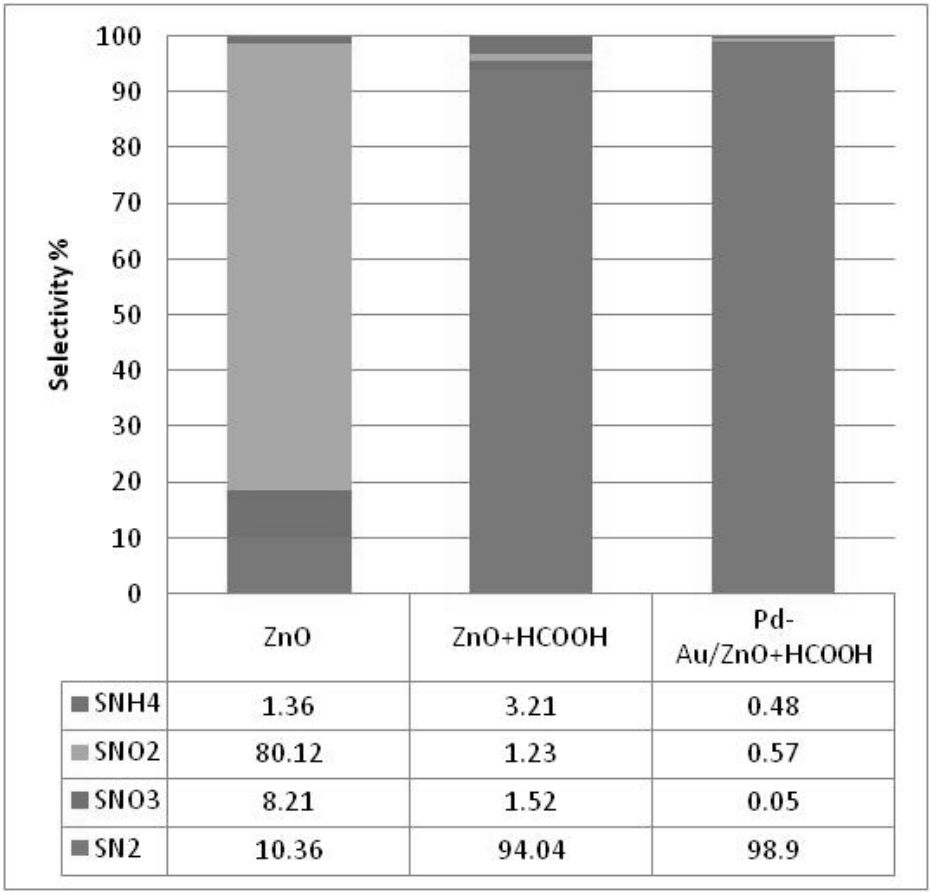

	ZnO	ZnO+HCOOH	Pd-Au/ZnO+HCOOH
SNH4	1.36	3.21	0.48
SNO2	80.12	1.23	0.57
SNO3	8.21	1.52	0.05
SN2	10.36	94.04	98.9

Fig. 8 – Selectivity to N_2, NO_2^-, $NH_4^+$and NO_3^- in photocatalytic reaction of nitrate reduction on ZnO and Pd-Au/ZnO nanoparticles after four hours (240) min.

CONCLUSIONS

The ZnO nanoparticles with a size of 100-150 nm with the wurtzite phase were synthetized by the green synthetic way with the extract of black tea in an alkaline medium.

Bimetallic nanoparticles Pd-Au of around 10 nm obtained in green way with the tannic acid were deposited on zinc oxide.

The pure ZnO and Pd-Au decorated ZnO were characterized by XRD, SEM-EDX, TEM, IR-spectroscopy and UV-Vis spectroscopy.

The photocatalytic performance of ZnO NPs and Pd-Au/ZnO deposited towards the removal of nitrate was evaluated both in the absence and presence of the formic acid as the reductant and/or hole scavenger. N_2 selectivity is dramatically enhanced by the presence of the formic acid as in the same experimental conditions.

REFERENCES

1. O. S. G. P. Soares, M. F. R. Pereira, J. J. M. Órfão, J. L. Faria and C. G. Silva. *Chem. Eng. J.* , **2014**, *251*, 123.
2. A. Sowmya and S. Meenakshi, *J. Water Proc. Eng.*, **2015**, *8*, 23.
3. B. K. Tiwari, N. P. Brunton and C. Brennan, "Handbook of Plant Food Phytochemicals: Sources, Stability and Extraction", John Wiley & Sons, 2013.
4. N. Wehbe, M. Jaafar, Ch. Guillard, J-M. Herrmann, S. Miachon, E. Puzenat and N. Guilhaume, *Appl. Catal. A: Gen*., **2009**, *368,*1.
5. F. A. La Porta, A. E. Nogueira, L. Gracia, W. S. Pereira, G. Botelho, T. A. Mulinari, J. Andrés and E. Longo, *J. Phys. Chem. Sol.*, **2017**, *103*, 179.
6. S. Park, H-J. Kim, J. S. Kim, K. Yoo, J. C. Lee, W. A. Anderson and J-H. Lee, *J. Nanosci. Nanotech.*, **2007**, *7,* 4069.
7. J. Choi, S. Chan, H. Joo, H. Yang and F. K. Ko, *Water Research*, **2016**, *101*, 362.
8. G. X. Zhu, Y. J. Liu, H. Xu, Y. Chen, X. P. Shen and Z. Xu, *Cryst. Eng. Comm.,* **2012**, *14,* 719.
9. Y. Z. Chen, D. Q. Zeng, K. Zhang, A. L. Lu, L. S. Wang, D. L. Peng, *Nanoscale*, **2014**, *6*, 874.
10. P. Li, Z. Wei, T. Wu, Q. Peng, Y. D. Li, *J. Am. Chem. Soc*., **2011**, *133* , 5660.
11. S. M. Saad, H. Hassan, I. Abdel-Shafy and M. S. M. Mansour, *Arabian J. Chem.*, **2016**, *in press.*
12. R. State, F. Papa, G. Dobrescu, C. Munteanu, I. Atkinson, I. Balint and A. Volceanov, *Env. Eng. Manag. J.*, **2015**, *14,* 587.
13. S. Mihaiu, J. Madarasz, G. Pokol, I. M. Szilagyi, T. Kaszas, O. C. Mocioiu, I. Atkinson, A. Toader, C. Munteanu, V. E. Marinescu and M. Zaharescu, *Rev.Roum.Chim.,* **2013**, *58,* 335.

14. Z. Wu, Z. Sheng, Y. Liu, H. Wang, N. Tang and J. Wang, *J. Hazard. Mater.*, **2009**, *164* ,542.
15. N. Udawatte, M. Lee, J. Kim, D. Lee, *ACS Appl Mater Interfaces*, **2011**, *3*, 4531.
16. J.-H Kim., H.-W. Chung, T. Randall *Lee, Chem. Matter*, **2006**, *18*, 4115.
17. D. A. Bulushev, S. Beloshapkin, J. R. H. Ross, *Catal. Today*, **2010**, *154*, 7.
18. M. Ojeda and E. Iglesia, *Angew. Chem. Int. Ed.* **2009**, *48*, 4800.
19. A. Garron and F. Epron, *Water Res*. **2005**, *39*, 3073.
20. J. Hirayama, R. Abe and Y. Kamiya, *Appl. Catal. B: Env.*, **2014**, *144*, 721.
21. J. Shi, C. Long and A. Li, *Chem. Eng. J.* , **2016***, 286,* 408.
22. M. Bowker, C. Morton and J. Kennedy, *J. Catal.*, **2014**, *310*, 10.